

## MUTUAL SOLUBILITIES OF COMPONENTS OF BINARY BLENDS OF *n*-OCTADECANE, DI-*n*-OCTYL ETHER, AND *N,N*-DIOCTYLAMINE

N.M. DJORDJEVIC and R.J. LAUB

*Department of Chemistry, San Diego State University, San Diego, CA 92182 (U.S.A.)*

(Received 4 April 1986)

### ABSTRACT

Differential scanning calorimetry (DSC) has been used to measure the solubilities, as well as finite-concentration activities and activity coefficients, of *n*-octadecane (OD) in *N,N*-dioctylamine (DOA) and di-*n*-octyl ether (DOE); and of DOA in DOE (of interest as extractants for rare-earth elements) by the method of solubility curves. Mixtures of OD+DOE show ideal solubility, viz.  $\log x = (A/T) + B$ ; where  $x$  is the limiting (saturation) mole fraction of the solute,  $A$  is related to the solute enthalpy of fusion, and  $B$  is a fitting constant. Blends of DOA+DOE exhibit positive deviations, while OD+DOA give both positive and negative deviations from solution ideality.

### INTRODUCTION

It has been known for very many years that a priori approximation of the solubility of non-electrolyte solids in liquids is possible for systems that conform to Raoult's law and, in addition, if the deviations are not too severe, for systems which do not conform as well [1–9]. For an ideal solution (or for only slightly non-ideal solutions), plots of the logarithm of the mole fraction ( $x$ ) corresponding to the limiting (i.e., saturation) solubility of the solute (the substance that separates as the solid phase) against the reciprocal of the absolute temperature ( $T$ ) to which the solubility pertains are straight lines whose slopes  $S$  correspond to  $\Delta H_f/2.3R$ , where  $\Delta H_f$  is the molar heat of fusion of the solid. Thus, limiting solubilities can be forecast as a function of  $T$  knowing only  $\Delta H_f$ . (If  $\Delta H_f$  varies with temperature the relation is only approximately linear, but the deviations are usually slight and can accordingly be neglected; see later.) The method is known as the technique of solubility curves, since the solid formed upon cooling the solution is presumed to be pure solute.

We have applied the solubility-curve technique in this work to the determination of the solubilities of *n*-octadecane (OD) in *N,N*-dioctylamine (DOA) and di-*n*-octyl ether (DOE); as well as DOA in DOE. The last two

compounds are of particular interest, as they are used both neat and in solution for the extraction of inorganic materials. For example, DOA has been employed for the extraction of uranium [10,11], thorium [12], niobium [13–15], tantalum [13], and osmium [16]; while DOE has been used for osmium [17].

## THEORY

We designate the solute as that component which, upon cooling of the system, precipitates first. We also specify that the solid phase is pure, i.e., that the solvent is neither soluble in, nor coprecipitates with, solid solute. The standard state of the solute is next defined as hypothetical pure supercooled liquid under its own saturation vapor pressure at the temperature  $T$  of the solution. Then, recalling the general condition for phase equilibrium,  $\mu_i^l = \mu_i^s$ , followed by substitution of appropriate expressions cast in terms of standard-state chemical potentials,

$$\mu_i^{0,l} + RT \ln x_i^l \gamma_i^l = \mu_i^{0,s} + RT \ln x_i^s \gamma_i^s \quad (1)$$

where  $x_i$  and  $\gamma_i$  are the mole fraction and activity coefficient, respectively, of solid (superscript s) or liquid (superscript l) components  $i$  at temperature  $T$ . Rearrangement of eqn. (1), followed by substitutions [8,9], subsequently yields the expression:

$$\ln(x_i^l \gamma_i^l / x_i^s \gamma_i^s) = -(\Delta H_f / RT)(1 - T/T_t) + (\Delta C_p / R)[\ln(T_t/T) - (T_t/T) + 1] \quad (2)$$

where  $T_t$  is the solute triple-point temperature.

If the melting point  $T_m$  of the solute is not more than 100 K above the solution temperature, the terms involving  $\Delta C_p$  can be neglected. Also,  $T_m$  can be substituted for  $T_t$  with little or no error introduced into the final result. In addition, since solid solute is presumed to be pure, the denominator of the log term tends to unity. Equation (2) therefore simplifies to:

$$\ln(x_i^l \gamma_i^l) = -(\Delta H_f / RT)(1 - T/T_m) \quad (3)$$

Equation (3) provides a reliable method for estimating solubilities in terms of measurable thermodynamic properties when the chemical nature of the solute is similar to that of the solvent, i.e., when  $\gamma^l$  approaches unity ("ideal" solubility). Plots of  $\ln x$  against  $T^{-1}$  are linear in such cases, where the slopes correspond to  $-\Delta H_f / R$ . However, when there are significant differences in the nature and size of the solute and solvent molecules, it is of course expected that  $\gamma_i^l \neq 1$ . For example,  $\gamma$  is generally greater than unity for the (nonpolar) components of solutions in which only dispersive forces are important; accordingly, the solute solubility is less than that correspond-

ing to ideal behavior, and plots of  $\ln x$  against  $T^{-1}$  have slopes more negative than  $\Delta H_f/R$ . In contrast, polar or specific chemical forces give rise to activity coefficients that are usually less than unity, which leads in turn to solubilities that are greater than those expected on the basis of the heat of fusion of the solute. Plots of  $\ln x$  against  $T^{-1}$  exhibit slopes that are less negative than ideal in these cases.

## EXPERIMENTAL

The differential scanning calorimeter was a Perkin-Elmer Model DSC-II, which was equipped with an Intracooler II. The latter permits subambient operation of the calorimeter, and consists of a compact mechanical refrigeration unit that is coupled to the DSC-II expansion chamber by means of an insulated flexible stainless-steel line. The accuracy of the temperature program was assessed with the melting points of indium (429.8 K) and *n*-octadecane (301.4 K); deviations were found to amount to no worse than  $\pm 1$  K. The heat of fusion of *n*-octadecane ( $57.7 \text{ cal g}^{-1}$ ) [18] was used as an absolute standard in determining the heats of fusion of DOA and DOE, as well as the thermal lag of the system. The heat capacity of sapphire was used as a standard for  $C_p$  measurements.

*N,N*-Dioctylamine (Fluka), di-*n*-octyl ether (Hardwicke Chemical Co.) and *n*-octadecane (Chemical Samples Co.) were vacuum-distilled prior to use. Samples of known composition of about 1.5–2.0 mg were weighed into aluminum pans, which were then crimped. A scanning rate of  $5^\circ \text{ min}^{-1}$  was used to cover a temperature interval of approximately  $50^\circ$  at a sensitivity setting of  $2 \text{ mcal s}^{-1}$ . Both the sample enclosure and the dry box of the Model DSC-II were purged with nitrogen during operation.

## RESULTS AND DISCUSSION

### *Properties of the pure compounds*

The observed molar enthalpies and entropies of fusion, together with the melting points of the pure compounds, are listed in Table 1. Also provided are the molar heat capacities of solid OD and DOA at 270 K and of DOE at 260 K; as well as the heat capacities of all three materials in the molten state at 315 K.

We found acceptable agreement, first, between the reported melting points and those observed experimentally both for DOA ( $T_{\text{obs}} = 286.1 \text{ K}$ ; 287 K reported [19]) and DOE ( $T_{\text{obs}} = 265.0 \text{ K}$ ; 265.4 K reported [20]). Secondly, the entropy of fusion of OD was appreciably higher than the values found either for DOE or DOA. We interpret this to be a reflection of

TABLE 1

Molar enthalpies  $\Delta H_f$  and entropies  $\Delta S_f$  of fusion; and molar heat capacities  $C_p$  of solid *n*-octadecane (OD; 270 K), *N,N*-dioctylamine (DOA; 270 K) and di-*n*-octyl ether (DOE; 260 K); and liquid OD, DOA and DOE (315 K)

Compound	MW (Da)	$T_m$ (K)	$C_p^s$ (cal mol <sup>-1</sup> K <sup>-1</sup> )	$C_p^l$ (cal mol <sup>-1</sup> K <sup>-1</sup> )	$\Delta H_f$ (kcal mol <sup>-1</sup> )	$\Delta S_f$ (e.u.)
OD	254.50	301.6	123.8	158.3	14.69	48.7
DOA	241.46	286.1	142.1	158.6	6.640	23.2
DOE	242.45	265.0	110.0	142.3	1.268	4.8

molecular ordering extent with the latter compounds: in general, rotational and translational degrees of freedom are acquired simultaneously on melting, e.g., as with OD. However, in some instances, as for molecules with large aspect (length-to-breadth) ratios and/or that are strongly associated, only translational motions are increased substantially upon melting, that is, rotational motions remain somewhat restricted. The entropy change upon melting for compounds of these types is therefore less than would otherwise be expected. The higher entropy of fusion for OD thus appears to indicate that DOE and DOA are more highly ordered in the liquid state. This may arise as a result, e.g., of self-association via hydrogen bonding.

#### *Properties of binary mixtures*

Tables 2–4 give the observed melting points of solutions of OD/DOA, OD/DOE, and DOA/DOE. Figures 1–3 then present the plots of  $\log x$  vs.  $1/T$  for the indicated systems. Least squares fitting was used to derive the coefficients  $A$  and  $B$  of the expression:

$$\log x = (A/T) + B \quad (4)$$

where the point  $(0, 1/T_m)$  was employed together with those data clearly

TABLE 2

Observed melting points  $T$  for indicated mole fractions  $x$  of *n*-octadecane (OD) + *N,N*-dioctylamine (DOA)

$x_{OD}$	$x_{DOA}$	$T$ (K)	$x_{OD}$	$x_{DOA}$	$T$ (K)
0.915	0.085	298.9	0.350	0.650	290.2
0.787	0.213	298.5	0.269	0.731	287.9
0.673	0.327	296.2	0.258	0.742	287.4
0.516	0.484	293.3	0.174	0.826	286.0
0.434	0.566	290.8	0.167	0.833	285.8
0.391	0.609	291.0	0.099	0.901	284.5
			0.043	0.957	285.0

TABLE 3

Observed melting points  $T$  for indicated mole fractions  $x$  of  $n$ -octadecane (OD)+ di- $n$ -octyl ether (DOE)

$x_{OD}$	$x_{DOE}$	$T$ (K)	$x_{OD}$	$x_{DOE}$	$T$ (K)
0.969	0.031	299.3	0.306	0.694	287.6
0.844	0.156	298.9	0.228	0.772	284.7
0.713	0.287	297.6	0.198	0.802	282.8
0.641	0.359	296.3	0.168	0.832	280.6
0.461	0.539	292.3	0.070	0.930	265.4
0.376	0.624	290.3	0.022	0.978	264.2

TABLE 4

Observed melting points  $T$  for indicated mole fractions  $x$  of  $N,N$ -dioctylamine (DOA)+ di- $n$ -octyl ether (DOE)

$x_{DOA}$	$x_{DOE}$	$T$ (K)	$x_{DOA}$	$x_{DOE}$	$T$ (K)
0.975	0.025	285.6	0.493	0.507	276.2
0.906	0.094	284.8	0.458	0.542	272.6
0.829	0.171	283.0	0.423	0.577	271.8
0.740	0.260	282.4	0.386	0.614	271.8
0.717	0.283	281.1	0.323	0.677	269.6
0.660	0.340	279.7	0.259	0.741	268.9
0.574	0.426	277.5	0.114	0.886	266.9
			0.004	0.996	266.3

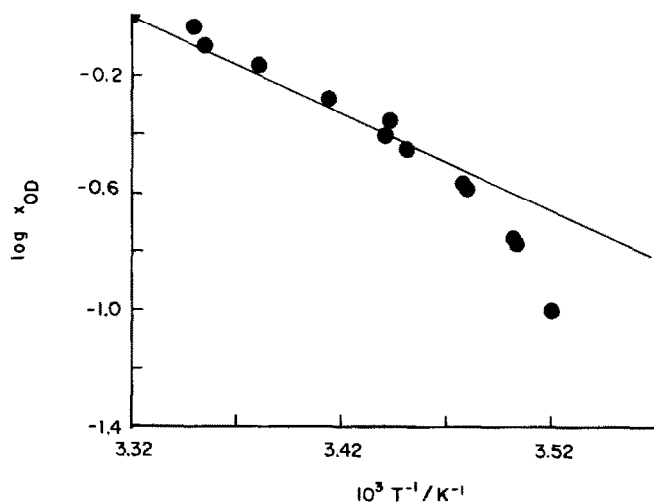


Fig. 1. Solubility-curve plot of  $\log x_{OD}$  against  $T^{-1}$  ( $K^{-1}$ ) for  $n$ -octadecane (OD) with  $N,N$ -dioctylamine (DOA). (●) observed values; (—) ideal ( $\gamma = 1$ ) solubility calculated with eqn. (3) and  $\Delta H_f$  of Table 1.

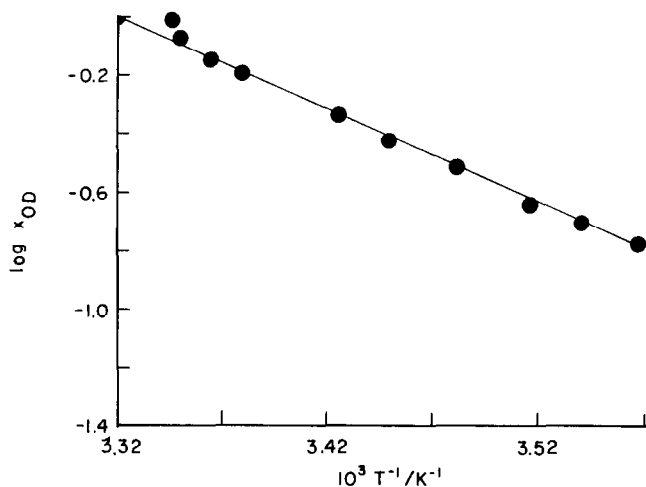


Fig. 2. As in Fig. 1; OD with di-*n*-octyl ether (DOE).

corresponding to the linear regions of the plots. Table 5 lists the values observed, the  $\Delta H_f$  calculated from the slopes  $A$ , and the temperature ranges over which linearity was found.

The apparent enthalpies of fusion for OD and DOA, derived from the respective solubility plots for OD with DOA and DOA with DOE, were substantially greater than those for the pure compounds (cf. Table 1), indicating that these systems deviate substantially from ideality. In contrast, the solubilities of OD in DOE were found to approximate ideal behavior over the temperature range 281–297 K. Further indication of this is pro-

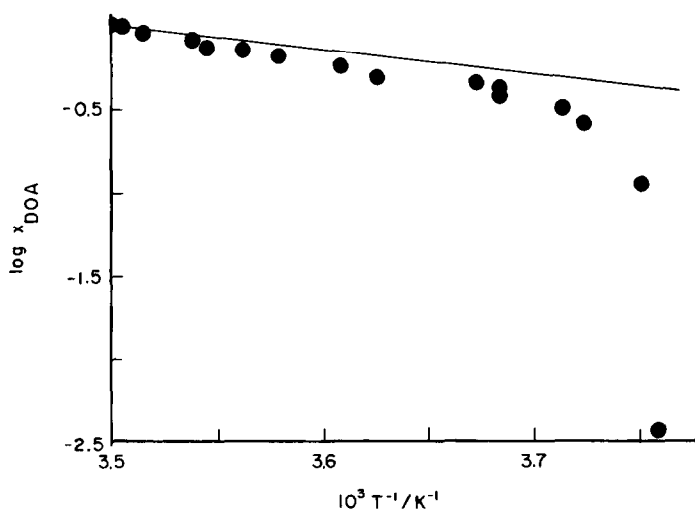


Fig. 3. As in Fig. 1; DOA with DOE.

TABLE 5

Best-fit constants (applicable over specified temperature-span  $\Delta T$  (K)) of eqn. (4) for indicated systems; and comparison of solute enthalpies of fusion  $\Delta H_f$  with those derived from the linear least-squares slopes

System	$\Delta T$ (K)	$B$	$-2.3RA$ (kcal mol <sup>-1</sup> )	$\Delta H_f$ (kcal mol <sup>-1</sup> )
OD/DOA	288–297	13.90	19.12	14.69
OD/DOE	281–297	10.59	14.62	14.69
DOA/DOE	266–285	7.817	10.25	6.640

TABLE 6

Activities  $a_{OD}$  of OD in DOA calculated with eqn. (3); smoothed limiting mole-fraction solubilities  $x_{OD}$  retrieved from eqn. (4) with fitting constants given in Table 5; and calculated solute activity coefficients  $\gamma_{OD} = a/x$

$T$ (K)	$a_{OD}$	$x_{OD}$	$\gamma_{OD}$
298.5	0.773	0.816	0.947
296.2	0.637	0.634	1.005
293.3	0.500	0.462	1.065
291.0	0.409	0.356	1.149
290.3	0.381	0.325	1.173
287.9	0.312	0.250	1.247
287.7	0.306	0.244	1.253
286.0	0.261	0.199	1.314

TABLE 7

Activities  $a_{OD}$  of OD in DOE calculated with eqn. (3); smoothed limiting mole-fraction solubilities  $x_{OD}$  retrieved from eqn. (4) with fitting constants given in Table 5; and calculated solute activity coefficients  $\gamma_{OD} = a/x$

$T$ (K)	$a_{OD}$	$x_{OD}$	$\gamma_{OD}$
298.9	0.802	0.806	0.994
297.6	0.715	0.720	0.993
296.3	0.642	0.647	0.993
292.3	0.458	0.462	0.991
290.3	0.384	0.388	0.990
287.6	0.303	0.307	0.989
284.7	0.233	0.236	0.987
282.8	0.195	0.197	0.987

vided in terms of the solute activities at the melting temperatures of the mixtures of Table 2, which were determined by putting the values of  $\Delta H_f$  and  $T_m$  (Table 1) into eqn. (3). The results are given in Tables 6–8. Also shown are the solute activity coefficients, which were calculated by retrieving (smoothed) values of  $x$  at the indicated temperatures from eqn. (4), and then dividing these into the respective activities.

TABLE 8

Activities  $a_{\text{DOA}}$  of DOA in DOE calculated with eqn. (3); smoothed limiting mole-fraction solubilities  $x_{\text{DOA}}$  retrieved from eqn. (4) with fitting constants given in Table 5; and calculated solute activity coefficients  $\gamma_{\text{DOA}} = a/x$

$T$ (K)	$a_{\text{DOA}}$	$x_{\text{DOA}}$	$\gamma_{\text{DOA}}$
285.6	0.981	0.961	1.021
284.8	0.949	0.913	1.039
283.0	0.880	0.813	1.083
282.4	0.858	0.782	1.097
281.1	0.811	0.717	1.132
279.7	0.767	0.658	1.167
277.5	0.696	0.566	1.230

The reversed-S curves for OD with DOA and DOE are thought to be due to two opposing contributions to deviations from Raoult's law [8]. On the one hand, differences in the polarities of the solute and solvent, which appear to be greatest at concentrations approaching pure OD, result in negative deviation with concomitant increased solubility. The opposing effect is due to differences in the internal pressures of the solution components, which is greatest at low concentrations of OD and which tends to counterbalance the effects of polarity.

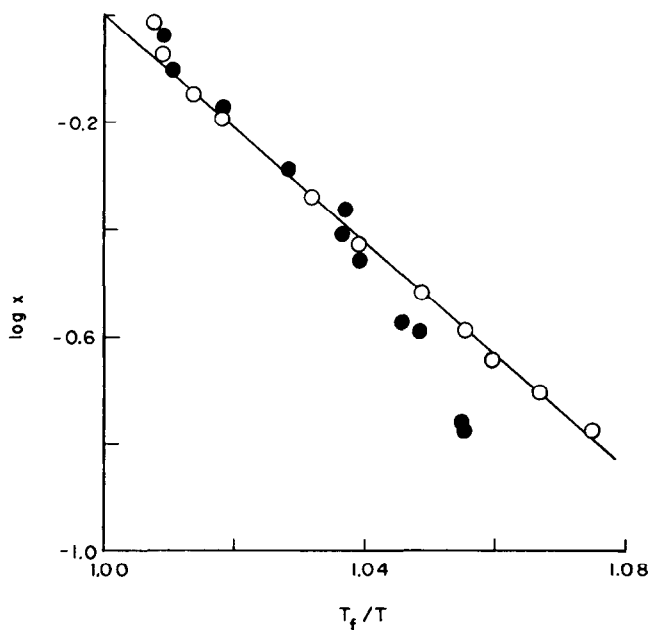


Fig. 4. Solubility curve plot of  $\log x_{\text{OD}}$  against reduced temperature  $T_f/T$  for DOA (●) and DOE (○) solvents. (—) ideal ( $\gamma = 1$ ) solubility calculated from  $\Delta S_f/R$  of Table 1.



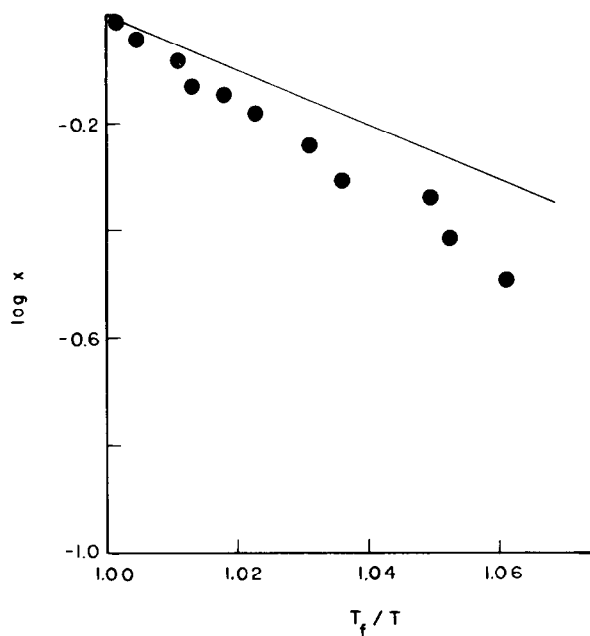


Fig. 5. As in Fig. 4; DOA solute with DOE solvent.

The results are illustrated further in Figs. 4 and 5, where  $\log x$  is plotted against a reduced temperature  $T_f/T$ ; where the ideal slope is  $\Delta S_f/R$  (solid lines in each figure). As mentioned earlier, both DOA and DOE are thought

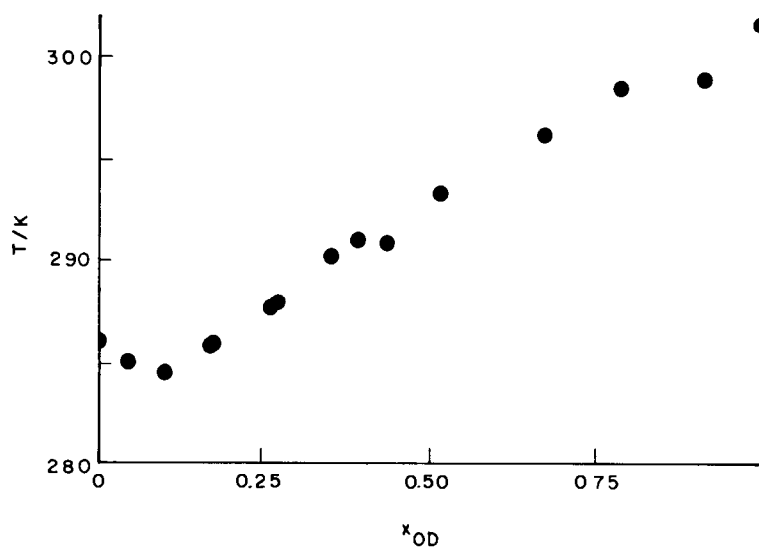


Fig. 6. Plot of temperature dependence of solubility of OD in DOA, showing eutectic points at 284, 291 (indistinct), and 299 K.

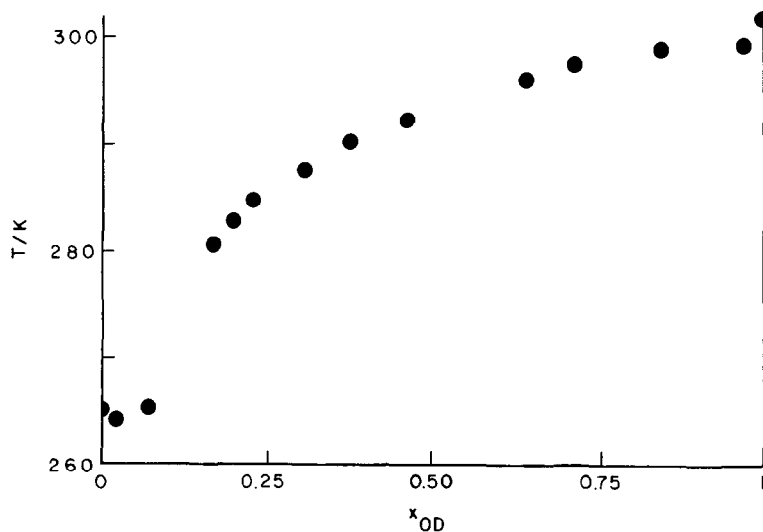


Fig. 7. As in Fig. 6; OD in DOE exhibiting eutectic points at 262 and 298 K.

to be dimerized to some extent at high concentration. However, whatever self-association there might be is likely destroyed upon dilution with (presumed-inert) OD. This results in an increase in the entropy of the system, which in turn lowers the free energy and, hence, which favors solubility. Thus, at  $(T_i/T)$  between 1 and 1.016 in Fig. 4,  $\gamma$  is less than unity and the solubility of OD in DOA as well as in DOE is greater than expected. Then,

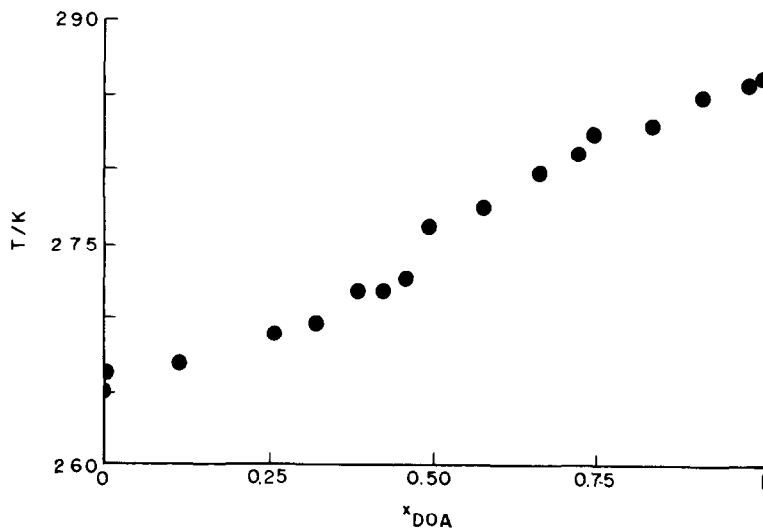


Fig. 8. As in Fig. 6; DOA in DOE (no distinct eutectic points).

as the concentration of OD is decreased the plots converge on ideality ( $\gamma = 1$ ). OD in DOA later diverges from ideality once more at  $T_f/T$  greater than ca. 1.04 (in fact, quite sharply so), i.e.,  $\gamma > 1$ , for which the solubility is less than expected.

For blends of DOA with DOE (Fig. 5)  $\gamma$  lies consistently greater than unity. That is, the solubility of DOA is less than expected, which would seem to preclude specific interactions with DOE at any composition.

The phase diagrams derived from Figs. 1–3 are presented in Figs. 6–8. These show eutectic points for mixtures of OD/DOA at 299, 291 (indistinct), and 284 K. Eutectic points were also found for blends of OD with DOE at 298 and 262 K. In contrast, DOA/DOE gave no clear indication of eutectic melting.

## CONCLUSIONS

Solubility curves of  $\log x$  against  $1/T$  have been used to measure deviations from (Raoult's law) ideality for chain-like systems, chosen such that any steric factors that might influence phase compositions or behavior were minimized. Mixtures of OD with DOE exhibited ideal solubility over the temperature range 297–281 K; while blends of OD with DOA gave both positive and negative deviations. Mixtures of DOA with DOE gave solute activity coefficients that were greater than unity over the entire temperature span evaluated and, thus, solubilities that were less than expected.

## ACKNOWLEDGMENT

Financial support provided for this work by the National Science Foundation is gratefully acknowledged.

## REFERENCES

- 1 I. Schroeder, *Z. Phys. Chem.*, 11 (1893) 449.
- 2 J.H. Hildebrand and C.A. Jenks, *J. Am. Chem. Soc.*, 42 (1920) 2180.
- 3 J.H. Hildebrand and C.A. Jenks, *J. Am. Chem. Soc.*, 43 (1921) 2172.
- 4 F.S. Mortimer, *J. Am. Chem. Soc.*, 44 (1922) 1416.
- 5 F.S. Mortimer, *J. Am. Chem. Soc.*, 45 (1923) 633.
- 6 H.L. Ward, *J. Phys. Chem.*, 30 (1926) 1316.
- 7 U.S. Rai, O.P. Singh, N.P. Singh and N.B. Singh, *Thermochim. Acta*, 71 (1983) 373.
- 8 J.H. Hildebrand and R.L. Scott, *The Solubility of Nonelectrolytes*, Dover Publications, New York, 3rd edn., 1964, Chap. XVII.
- 9 J.M. Prausnitz, *Molecular Thermodynamics of Fluid-Phase Equilibria*, Prentice-Hall, Englewood Cliffs, NJ, 1969, Chap. 9.

- 10 T. Sato, *Bull. Chem. Soc. Jpn.*, 41 (1968) 99.
- 11 A.M. Rozen and Z.I. Nagnibeda, *Radiokhimiya*, 13 (1971) 284.
- 12 T. Sato, *J. Inorg. Nucl. Chem.*, 32 (1970) 1341.
- 13 I.P. Alimarin, I.M. Gibalo, N.A. Ivanov and E.A. Sanaeve *Radiokhimiya*, 11 (1969) 515.
- 14 N.A. Ivanov, I.P. Alimarin, I.M. Gibalo and G.F. Bebikh, *Izv. Akad. Nauk. SSSR, Ser. Khim.*, 12 (1970) 2664.
- 15 I.P. Alimarin, N.A. Ivanov and I.M. Gibalo, *Izv. Akad. Nauk. SSSR, Ser. Khim.*, 13 (1971) 475.
- 16 H. Meler, E. Zimmerhackl, W. Albrecht, D. Boesche, W. Hecker, P. Menge, A. Ruckdeschel, E. Unger and G. Zeitler, *Mikrochim. Acta*, 4 (1969) 826.
- 17 H. Meler, E. Zimmerhackl, W. Albrecht, D. Boesche, W. Hecker, P. Menge, A. Ruckdeschel, E. Unger and G. Zeitler, *Mikrochim. Acta*, 4 (1969) 839.
- 18 A.A. Schaerer, *J. Am. Chem. Soc.*, 77 (1957) 2017.
- 19 V.S. Zakharkin, V.I. Zemlyanukhin and V.B. Shevchenko, *Radiokhimiya*, 12 (1970) 577.
- 20 D.W. Lawrence and G.W. Pania, *J. Am. Chem. Soc.*, 75 (1953) 4836.